ARTICLE   OPEN

Check for updates

Connectome dysfunction in patients at clinical high risk for psychosis and modulation by oxytocin

Cathy Davies [1,2,3,14✉], Daniel Martins [3,4,5,14], Ottavia Dipasquale[3], Robert A. McCutcheon[2,6], Andrea De Micheli[1,7], Valentina Ramella-Cravaro[1], Umberto Provenzani[1,8], Grazia Rutigliano[1], Marco Cappucciati[1], Dominic Oliver [1,6], Steve Williams [3], Fernando Zelaya[3], Paul Allen[3], Silvia Murguia[9], David Taylor[10], Sukhi Shergill[2,11], Paul Morrison[2], Philip McGuire [6,12,13], Yannis Paloyelis [3,15] and Paolo Fusar-Poli [1,4,7,8,15]

Abnormalities in functional brain networks (functional connectome) are increasingly implicated in people at Clinical High Risk for Psychosis (CHR-P). Intranasal oxytocin, a potential novel treatment for the CHR-P state, modulates network topology in healthy individuals. However, its connectomic effects in people at CHR-P remain unknown. Forty-seven men (30 CHR-P and 17 healthy controls) received acute challenges of both intranasal oxytocin 40 IU and placebo in two parallel randomised, double-blind, placebo-controlled cross-over studies which had similar but not identical designs. Multi-echo resting-state fMRI data was acquired at approximately 1 h post-dosing. Using a graph theoretical approach, the effects of group (CHR-P vs healthy control), treatment (oxytocin vs placebo) and respective interactions were tested on graph metrics describing the topology of the functional connectome. Group effects were observed in 12 regions (all $p_{FDR} < 0.05$) most localised to the frontoparietal network. Treatment effects were found in 7 regions (all $p_{FDR} < 0.05$) predominantly within the ventral attention network. Our major finding was that many effects of oxytocin on network topology differ across CHR-P and healthy individuals, with significant interaction effects observed in numerous subcortical regions strongly implicated in psychosis onset, such as the thalamus, pallidum and nucleus accumbens, and cortical regions which localised primarily to the default mode network (12 regions, all $p_{FDR} < 0.05$). Collectively, our findings provide new insights on aberrant functional brain network organisation associated with psychosis risk and demonstrate, for the first time, that oxytocin modulates network topology in brain regions implicated in the pathophysiology of psychosis in a clinical status (CHR-P vs healthy control) specific manner.

Molecular Psychiatry; https://doi.org/10.1038/s41380-024-02406-x

INTRODUCTION

Abnormal functional connectivity is one of the strongest biological markers associated with psychosis [1–3]. Alterations in the brain's functional network organisation (functional connectome) are also observed prior to the onset of psychosis in people at Clinical High Risk (CHR-P) [4–6]. These help-seeking individuals present with attenuated psychotic symptoms, emotional, cognitive and functional impairments and have a 20% two-year risk of transitioning to frank psychosis [7, 8]. There are currently no licensed pharmacological treatments for CHR-P patients [9, 10], which represents a significant unmet clinical need. A deeper understanding of the connectomic abnormalities contributing to psychosis risk, and the potential ameliorative effects of experimental therapeutics, is urgently required.

Accumulating evidence from different imaging modalities has revealed brain-wide as well as regional dysfunction in people at CHR-P [11, 12] and those with established psychosis (for reviews see [13, 14]), particularly in the hippocampus, striatum, thalamus and frontal cortex—core components of the most influential circuit models of psychosis pathophysiology [15–17]. Evidence of aberrant resting-state functional connectivity between brain regions [18–20] subsequently highlighted that psychosis-related dysfunction cannot entirely be described by spatially discrete differences in neural activation. Psychosis-related dysconnectivity can be identified both within and between large-scale networks, particularly involving frontoparietal, default mode and salience networks [21–23]. This suggests that network-based approaches are needed to fully capture the

complete spectrum of brain dysfunction associated with psychosis.

More recently, the application of graph theory [24] to neuroimaging data opened up new possibilities for exploring aberrant functional brain network organisation from micro-to-macro-scale levels of analysis [25]. Using graph theory, brain regions are represented by nodes, the functional connections between nodes represented by edges, and modules defined as communities of highly intra-connected nodes that have fewer inter-module connections [26]. Like any complex network, the topology (organisational properties) of the human brain shapes its capacity for information transfer, influencing higher-order functions such as cognition as well as its vulnerability to insult [25, 27, 28]. A disruption to the finely-tuned balance of integration vs segregation may lead to loss of high-fidelity information transfer, cognitive dysfunction and the psychotic phenomenology characteristic of the CHR-P state and frank psychosis [1, 26, 29]. Supporting this hypothesis, evidence suggests that people with established psychosis have abnormalities across global and local (node- or module-level) topological properties [26], including reduced small-worldness [30], clustering [31], hubness [32] and modularity [33], as well as changes in global and local efficiency [2]. However, the network dysfunction that precedes psychosis onset in the CHR-P state is less well characterised.

The few studies conducted to date have shown that abnormal modular organisation in CHR-P individuals at baseline is associated with a three-fold transition rate to frank psychosis [4]. Further work demonstrates that CHR-P individuals who go on to transition (vs controls and non-transitions) have altered topological centrality in frontal and anterior cingulate regions [5], reduced global efficiency and clustering [6] (although global differences are not always found in this population [5, 34]), regional changes in nodal efficiency correlating with symptom severity [6], and extensive reorganisations of network community structure across most of the large-scale resting-state networks [6]. Together, these data suggest that further mapping of CHR-associated functional connectomic alterations—and how they respond to experimental therapeutics—would not only enrich understanding of the neurobiological mechanisms driving psychosis onset but may also illuminate novel treatment targets.

One potential novel treatment is the neuropeptide oxytocin, which has neurobehavioural effects in multiple domains that could be beneficial for CHR-P individuals. These include anxiolytic effects [35], modulation of social-emotional cognition [36] and hypothalamic-pituitary-adrenal axis regulation [35]. In our previous work we demonstrated that oxytocin modulates frontal activation during mentalising [37], anterior cingulate neurochemistry [38] and resting cerebral blood flow in the hippocampus among numerous other regions [39] in people at CHR-P. Independent evidence further suggests that oxytocin modulates connectivity within resting-state networks in healthy volunteers [40, 41] and 'normalises' aberrant connectivity in several clinical populations, including patients with social anxiety [42], post-traumatic stress disorder [43] and autism [44]. Moreover, a recent study in healthy males demonstrated that a single dose of oxytocin was sufficient to modulate local functional network topology, including in regions and networks implicated in psychosis risk [45]. This raises the possibility that oxytocin may ameliorate the connectomic dysfunction present in CHR-P individuals. Interestingly, although the oxytocin system has not been fully elucidated in humans, preclinical work shows that oxytocin targets fast-spiking GABAergic interneurons to enhance the fidelity and temporal precision of spike transmission, thus augmenting signal-to-noise ratio in information transfer across brain networks [46]. This is just one of a number of potential mechanisms [47] relevant to psychosis pathophysiology [15] through which oxytocin may modulate functional network topology. It is unclear, however, whether oxytocin will have

similar connectomic effects in CHR-P patients as previously observed in healthy controls. Supporting the hypothesis that a differential effect may exist is our recent finding that oxytocin increases cardio-parasympathetic activity in CHR-P but not healthy males [48].

To address this gap, in this study we took a data-driven approach combining multi-echo resting-state blood-oxygen-level-dependent (BOLD) functional magnetic resonance imaging (fMRI) with graph-theory modelling. We investigated differences in global and regional topology of the functional connectome related to (a) CHR-P status (CHR-P patients vs controls; group effects), (b) the main effects of intranasal oxytocin vs placebo (treatment effects), and (c) group x treatment interactions to identify clinical status-specific effects of oxytocin.

SUBJECTS & METHODS
Participants
Thirty male, help-seeking CHR-P individuals aged 18–35 were recruited from a specialist early detection service in London, UK. A CHR-P status was determined using the Comprehensive Assessment of At-Risk Mental States (CAARMS) 12/2006 criteria. Seventeen healthy male controls, aged 19–34, were recruited as part of a related study (see below) [45]. Full inclusion and exclusion criteria, sample size details, justification and comparison of the current vs previously published control data are detailed in the Supplementary Methods. In both studies, subjects were asked to abstain from using recreational drugs for at least 1 week and alcohol for at least 24 h prior to each session. Urine screening was conducted before each session. The study received Research Ethics approval (London Bridge Committee: 14/LO/1692 and King's College London Committee: PNM/13/14-163) and all subjects gave written informed consent.

Design, materials, procedure
CHR-P and control data were combined from two related studies which were collaboratively designed so that their data could be analysed together. The CHR-P study (ISRCTN48799530) used a randomised, double-blind, single-dose challenge of intranasal oxytocin versus placebo in a crossover design (one-week wash-out), as previously reported [37–39, 48]. Participants self-administered 40 IU intranasal oxytocin or placebo using a standard nasal spray, as per our in-house protocol [49] following recommended guidelines (Supplementary Materials) [50]. Participants were randomly allocated to a treatment order (oxytocin/placebo or placebo/oxytocin). Following drug administration, participants underwent a battery of MRI sequences which started in the morning period to minimise potential effects of diurnal variation in oxytocin levels [51]. Healthy control data came from a related randomised, double-blind, single-dose triple-dummy crossover study [45], where participants received oxytocin/placebo via three administration routes (nasal spray, nebulizer and intravenous infusion) in one of two fixed sequences: either nebulizer/intravenous/spray, or spray/intravenous/nebulizer. In three out of four sessions only one route of administration contained the active drug; in the fourth session, all routes delivered placebo or saline. The dose administered intranasally was 40 IU. For this study, we only used data from the placebo and nasal spray arms to maximise comparability to the protocol used in the CHR-P sample. Therefore, dose, device for drug administration, scanner and time post-dosing were matched across studies.

MRI acquisition, preprocessing and denoising
All scans were conducted on a General Electric Discovery MR750 3 Tesla system (General Electric, Chicago, USA) using a 32-channel head coil. The 8 min 10 s multi-echo resting-state fMRI scan was obtained starting at (M±SD) 62.6±3.1 min post-dosing in the CHR-

P group and 57.01 ± 3.38 min in healthy controls. Acquisition parameters, image preprocessing and denoising procedures (performed using the AFNI tool MEICA.py [52, 53]) are detailed in the Supplementary Methods.

Functional connectivity

Figure 1 provides an overview of the network analysis steps. To generate brain-wide functional connectivity matrices for each subject and treatment condition, we first extracted the BOLD time courses for each anatomical region-of-interest (ROI) for each participant/session using *fslmeants* from the FMRIB Software Library (FSL). We used the Desikan-Killiany atlas (66 cortical regions) [54] together with the 9 bilateral subcortical regions (cerebellum, thalamus, caudate, putamen, pallidum, hippocampus, amygdala, accumbens, ventral diencephalon) and brainstem from the Harvard-Oxford Atlas. This combination offers good cortical-subcortical coverage and both atlases have been used extensively (and often together) in previous work [28, 55–58], aiding the interpretation and comparability of findings. Signal dropout in the bilateral frontal pole meant that these 2 nodes were removed, leaving 83 nodes. We generated bivariate Pearson's correlation matrices for the time courses of all possible pairs of ROIs (83×83) using Matlab/R2015b. Supplemental analyses using partial correlation matrices, which may reflect more direct connections [59], were calculated using FSLnets with Tikhonov's regularisation (coefficient 0.1) and are appended in the Supplementary Material. Finally, we normalised our correlation measures to z-scores using the Fisher r-z transform. To ensure that any graph metric results were not driven by patient-control differences in overall connectivity strength [60], we examined mean functional connectivity, calculated as the average of the elements in the lower triangular matrix for each subject/condition.
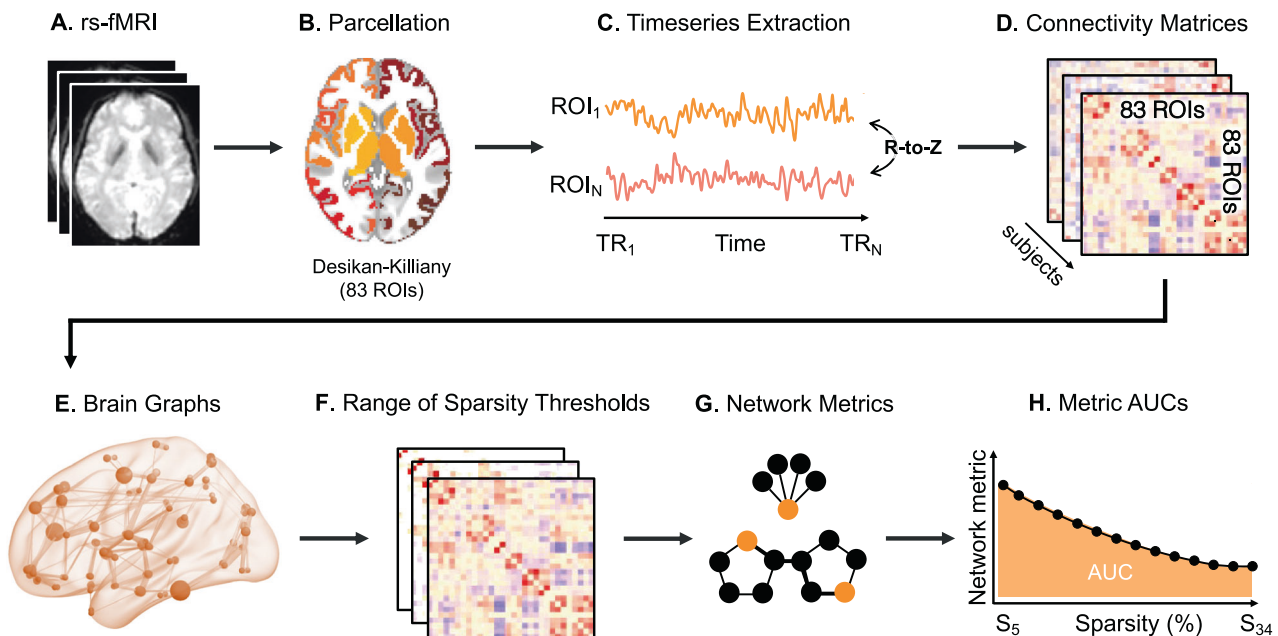
Graph estimation and network characterisation

Our z-transformed connectivity matrices were then used to construct brain graphs representing the functional connectome for each subject/condition, using an undirected signed weighted approach [27]. From the fully weighted networks we calculated equi-sparse networks by retaining a fixed percentage (K) of the total amount of possible edges. In order to determine systematic differences in the network's topological organisation that are not dependent on the choice of an arbitrary threshold, we chose a range of sparsity thresholds from 5 to 34%, with steps of 1%, based on previous evidence showing the characteristic small-world behaviour of human brain networks is most consistently observed for this range [61]. For each brain network and sparsity level, we used the Matlab functions provided with the Brain Connectivity Toolbox [27] to compute one global (global efficiency) and three nodal network metrics: betweenness-centrality, local efficiency and node degree. Details on the calculation of each of these metrics have been described elsewhere [27] but a brief overview is provided in Supplementary Figure S1. For each of the graph metrics analysed, we summarised the different values over the range of thresholds using the area under the curve (AUC), providing a summary estimator for each graph metric that is independent of single threshold selection and which is sensitive to topological differences in brain networks [62]. All of our statistical analyses on graph metrics were therefore run on AUC parameters rather than the raw values.

Statistical analysis

We investigated group differences, treatment effects and (group x treatment) interactions across micro-to-macro-scale levels of functional connectome organisation. Specifically, we examined mean connectivity strength and global efficiency of the whole-brain network, the three nodal graph metrics, and individual connections between pairs of nodes. To evaluate the main effect of group (i.e. differences related to CHR-P status), treatment conditions were collapsed by calculating a mean average per subject and 2-sample t-tests conducted. For the main effect of treatment, oxytocin minus placebo (difference) values were calculated per subject and one-sample t-tests conducted. To examine interactions, the difference values were entered into two-sample (CHR-P vs control) t-tests. These analyses were conducted in Matlab and the directionality of significant interactions was determined by examining subject-level values.

Global metrics. We calculated mean connectivity strength and global efficiency of the brain network for each participant and treatment condition and compared groups, treatments and interactions using the relevant t-tests, as above. Group differences

A. rs-fMRI **B.** Parcellation **C.** Timeseries Extraction **D.** Connectivity Matrices

Desikan-Killiany
(83 ROIs)

ROI₁ ROIₙ R-to-Z TR₁ Time TRₙ

83 ROIs

subjects

E. Brain Graphs **F.** Range of Sparsity Thresholds **G.** Network Metrics **H.** Metric AUCs

Network metric Sparsity (%) AUC S₅ S₃₄

Fig. 1 Schematic overview of the network analysis steps.

in mean connectivity during the placebo condition (only) were also examined with a 2-sample t-test.

Node level metrics. We retrieved values for the betweenness-centrality, local efficiency and degree of each node of the connectome for each subject and treatment condition. Average and difference values were computed (as above) to examine the main effects of group, treatment and interaction effects using t-tests (as above), controlling false positives with FDR correction for the number of nodes examined. Significance set at $p_{FDR} < 0.05$. Supplementary analyses comparing the groups' placebo conditions alone were conducted using 2-sample t-tests.

Results were visualised using ENIGMA toolbox v2, MRIcron and BrainNet Viewer. In the main text visualisation, all significant results were presented together on one brain template irrespective of the metric (betweenness-centrality, node degree and local efficiency), by assigning all significant t-statistics to their respective regions across metrics. Where there were effects in the same region in more than one metric, the larger t-value was shown. Further supplementary visualisations depicted results by individual metrics.

Edge level metrics. To investigate differences in each individual edge of the connectivity matrices, we used the Network Based Statistics (NBS) method [63] implemented in the NBS toolbox v1.2 to control the family-wise error rate (in the weak sense) when mass-univariate testing is performed at every edge of the graph. While this approach does not allow for inferences on individual connections, it allows extraction of subnetworks or topological clusters of regions that are significantly differently connected between groups and conditions [63]. When compared to analyses at the individual edge level, the NBS method offers greater sensitivity while also controlling for false positives [63]. In our NBS analysis, we tested for effects of group, treatment and interactions each using three arbitrary primary thresholds: 1.5, 3.1 and 4. We then used a two-tailed significance threshold of p < .05, with 5000 permutations.

Overlap with large-scale resting-state networks

To maximise the interpretability of our findings and facilitate comparisons with previous work focusing on large-scale resting-state networks (RSNs) [40, 45], we quantified the percentage of overlap (Dice-kappa coefficient) between our group, treatment and interaction effect maps (separately) and each of the RSNs described in the atlas from Yeo et al. [64], as detailed in the Supplementary Material. These values provide a qualitative contextualisation of our main findings which the reader can use for quick comparisons with previous literature.

RESULTS
Sample characteristics

Demographic and clinical characteristics of the sample are presented in Table 1. There were significantly more smokers in the CHR-P relative to the control group. One CHR-P subject was removed due to protocol violations and another omitted due to excessive head movement, leaving a sample of 28 CHR-P individuals and 17 controls.

Main effect of group (CHR-P vs healthy controls)

Global metrics. There was no main effect of group (t(43) = –0.86, p = 0.39), nor any difference between groups when comparing the placebo conditions alone (t(43) = –0.82, p = 0.42) on mean functional connectivity. There were no significant group effects (t(43) = –1.59, p = 0.12) on global efficiency.

Betweenness-centrality. Across conditions (oxytocin and placebo conditions combined), compared to healthy controls, CHR-P individuals had lower betweenness-centrality of the left caudal middle frontal gyrus and left insula, but greater betweenness-centrality of the right inferior and superior temporal gyri.

Nodal degree. CHR-P individuals had lower node degree of the left lingual gyrus compared to controls, but greater node degree of the right lateral orbitofrontal cortex and right pars triangularis.

Table 1. Participant demographic and clinical characteristics.

Variable	CHR-P (N = 30)	Controls (N = 17)	Statistics
Age, years; mean (SD)	23.2 (4.7)	24.2 (5.3)	p = 0.51[c]
Sex, N (%) male	30 (100)	17 (100)	N/A[d]
Ethnicity, N White/Black/Asian/Mixed	16/6/4/4	–	–
Handedness, N (%) right	26 (87)	17 (100)	p = 0.15[e]
Education, years; mean (SD)	13.2 (1.9)[g]	–[g]	–
CHR-P Subtype[a], N BLIPS/APS/GRD	6/23/1	N/A	N/A
CAARMS positive symptoms[b]; mean (SD)	11.7 (3.3)	N/A	N/A
GF social score; mean (SD)	6.8 (1.5)	N/A	N/A
GF role score; mean (SD)	7.0 (1.7)	N/A	N/A
Current smoker, N (%) yes	17 (57)	4 (24)	p = 0.028[f]
Cigarettes/day; mean (SD)	9.8 (6.0)	4.5 (4.0)	p = 0.12[c]
Cannabis ever used, N (%) yes	24 (80)	10 (59)	p = 0.18[e]
Current alcohol use, N (%) yes	26 (87)	16 (94)	p = 0.64[e]

[a]CAARMS Comprehensive Assessment of At-Risk Mental States subgroup, BLIPS Brief Limited Intermittent Psychotic Symptoms, APS Attenuated Psychotic Symptoms, GRD Genetic Risk and Deterioration.
[b]Sum of the global (severity) ratings for positive subscale items (P1-P4) of the CAARMS. GF - Global Functioning (Role and Social) Scale.
[c]Independent t test.
[d]No statistical test necessary.
[e]Fisher's Exact test.
[f]chi-square test.
[g]The majority of controls were university students (approximately between 13 and 16 years of education), whereas 43% of CHR-P were university students or had completed a degree—of the remaining CHR-P subjects, 27% were currently undertaking A-Levels/BTEC (11–13 years of education), 20% were in full-time or part-time work, and 10% were unemployed.

Local efficiency. Compared to controls, CHR-P individuals had greater local efficiency of the bilateral pericalcarine cortex, bilateral rostral middle frontal gyrus and right pars orbitalis. There were no regions where local efficiency was significantly greater in controls vs the CHR-P group.

Details of significant nodal metric results are presented in Table 2 and Fig. 2, with metric-level figures appended in Fig S2.

Results of supplementary analyses comparing the groups' placebo conditions alone are presented in Supplementary Table S1.

Subnetworks. The NBS analyses did not identify any subnetworks where there were significant effects of group on connectivity after correcting for multiple testing, irrespective of the primary threshold used.

Table 2. Effects of group, treatment and interaction effects on nodal betweenness-centrality, degree and local efficiency.

Group effects			
Node	**Direction**	**T statistic**	**P (FDR-corr)**
Betweenness-Centrality			
Caudal middle frontal gyrus, left	HC > CHR	−2.165	0.036
Insula, left	HC > CHR	−2.236	0.031
Inferior temporal gyrus, right	CHR > HC	2.150	0.037
Superior temporal gyrus, right	CHR > HC	2.092	0.042
Node degree			
Lingual gyrus, left	HC > CHR	−2.217	0.032
Lateral orbital frontal cortex, right	CHR > HC	2.757	0.009
Pars triangularis, right	CHR > HC	2.353	0.023
Local efficiency			
Pericalcarine cortex, left	CHR > HC	2.451	0.018
Rostral middle frontal gyrus, left	CHR > HC	3.896	<0.001
Pars orbitalis, right	CHR > HC	2.698	0.010
Pericalcarine cortex, right	CHR > HC	2.125	0.039
Rostral middle frontal gyrus, right	CHR > HC	2.142	0.038
Treatment effects			
Node	**Direction**	**T statistic**	**P (FDR-corr)**
Betweenness-Centrality			
Brainstem	OT > PL	2.337	0.024
Supramarginal gyrus, left	PL > OT	−2.249	0.030
Insula, right	PL > OT	−3.286	0.002
Node degree			
Precentral gyrus, left	OT > PL	2.885	0.006
Local efficiency			
Paracentral lobule, left	OT > PL	2.699	0.010
Paracentral lobule, right	OT > PL	2.652	0.011
Pars opercularis, right	OT > PL	2.600	0.013
Interaction effects			
Node	**Direction**	**T statistic***	**P (FDR-corr)**
Betweenness-centrality			
Precentral gyrus, right	OT > PL in CHR; OT < PL in HC	2.062	0.045
Thalamus, left	OT > PL in CHR; OT < PL in HC	2.059	0.046
Pallidum, right	OT > PL in CHR; OT < PL in HC	2.785	0.008
Precuneus cortex, left	OT < PL in CHR; OT > PL in HC	−3.387	0.002
Superior frontal gyrus, left	OT < PL in CHR; OT > PL in HC	−2.561	0.014
Accumbens, left	OT < PL in CHR; OT > PL in HC	−2.490	0.017
Node degree			
Precuneus cortex, left	OT < PL in CHR; OT > PL in HC	−2.437	0.019
Superior frontal gyrus, left	OT < PL in CHR; OT > PL in HC	−2.139	0.038
Local efficiency			
Entorhinal cortex, left	OT > PL in CHR; OT < PL in HC	2.247	0.030
Entorhinal cortex, right	OT > PL in CHR; OT < PL in HC	2.633	0.012
Temporal pole, right	OT > PL in CHR; OT < PL in HC	2.102	0.041
Pericalcarine cortex, left	OT < PL in CHR; OT > PL in HC	−2.061	0.045

FDR-corr indicates FDR-corrected *P* values. *Interaction *t* test compared difference values (oxytocin minus placebo) between groups.
OT oxytocin, *PL* placebo, *CHR* Clinical High Risk for Psychosis, *HC* healthy control.
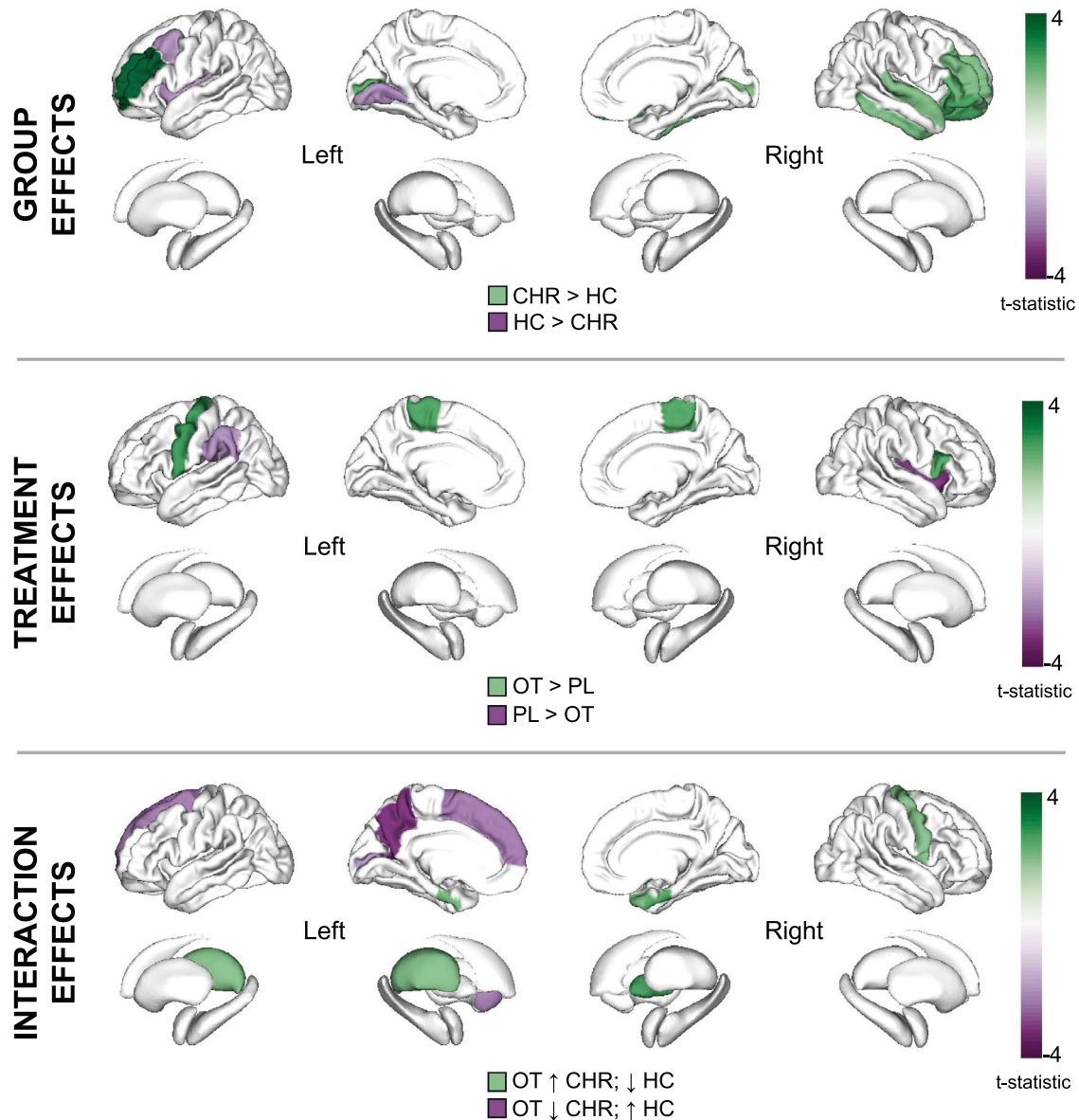
Fig. 2 Overview of group, treatment and interaction effects across all nodal metrics (betweenness-centrality, node degree and local efficiency). The shade of colour represents the t-statistic for each region. Only regions surviving FDR-corrected significance threshold $p < 0.05$ shown. In the top panel depicting main effects of group, regions in purple and green depict lower and greater graph metrics (respectively) in CHR-P relative to healthy controls (HC). In the middle panel depicting treatment effects, regions in green and purple depict increases and decreases (respectively) in graph metrics under oxytocin (OT) relative to placebo (PL). Although significant, the brainstem (t = 2.34) is not depicted as it is not included in the ENIGMA visualisation template. In the lower panel depicting group x treatment interaction effects, regions in green depict where oxytocin increased (↑) graph metrics in the CHR-P group but decreased (↓) them in healthy controls; regions in purple depict where oxytocin decreased graph metrics in the CHR-P group but increased them in controls. All results are presented here irrespective of the metric; where there were effects in the same region in more than one nodal metric, the larger t-value is shown. All corresponding statistics are presented in Table 2 and individual figures for each metric are appended in Supplementary Figs. 2–4.

Overlap with RSNs. The pathways for which we identified significant nodal differences between CHR-P individuals and controls overlapped primarily with regions belonging to the frontoparietal network (Dice coefficient = 0.58) and to a lesser extent, the limbic network (Dice coefficient = 0.26). The overlap with other networks was numerically weaker. All overlap findings are displayed in Fig. 3.

Main effect of treatment (oxytocin vs placebo)
Global metrics. There were no significant treatment effects on mean functional connectivity (t(44) = 1.27, $p = 0.21$) nor global efficiency (t(44) = 0.44, $p = 0.66$).

Betweenness-centrality. Over all individuals (CHR-P and controls combined), compared to placebo, oxytocin increased the betweenness-centrality of the brainstem, while it decreased the betweenness-centrality of the left supramarginal gyrus and right insula.

Nodal degree. Compared to placebo, oxytocin increased node degree of the left precentral gyrus. There were no regions where oxytocin decreased node degree.

Local efficiency. Compared to placebo, oxytocin increased the local efficiency of the bilateral paracentral lobule and the right
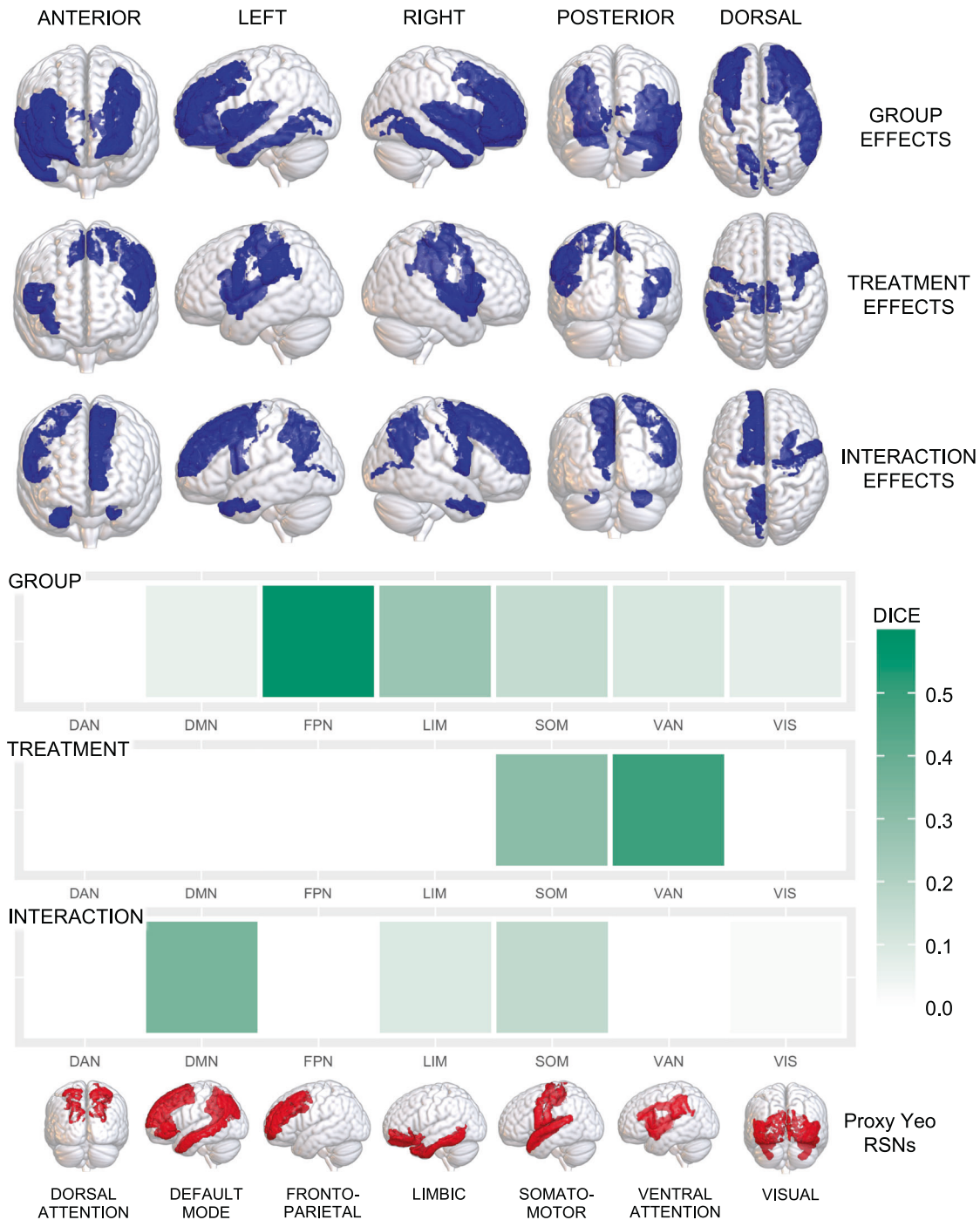
Fig. 3 Overlap between the group, treatment and interaction findings and the large-scale canonical resting-state networks (RSNs). We calculated the percentage of overlap between our result maps—which included binary masks of all cortical regions showing differences in nodal metrics (for group, treatment and interaction effects, separately)—and the large-scale RSNs described in the atlas from Yeo et al. [64]. As subcortical structures are not covered by the Yeo atlas, these were omitted from our result maps to prevent artificial reduction of the overlap estimate. The Yeo atlas includes a coarse parcellation of 7 canonical RSNs: the default-mode (DMN), dorsal attention (DAN), frontoparietal (FPN), limbic (LIM), somatomotor (SOM), visual (VIS) and ventral attention (VAN) networks. We created a proxy DKA>Yeo atlas for each of the 7 Yeo RSNs by combining individual DKA regions, allocating each to a single RSN based on the RSN for which each region had the highest number of overlapping vertices based on the confusion matrix from a previous study [100]. Overlap was quantified using the Dice-kappa coefficient, which measures the percentage of voxels of each RSN overlapping with our group/treatment/interaction effect maps. In the upper section, we provide an overview of all regions where we found group, treatment or interaction effects, irrespective of the specific graph metric, rendered in a 3D glass brain (semi-transparent) surface model. In the lower section, we provide a heatmap summarising the percentage of overlap (Dice-kappa coefficient) between our results and each of the 7 networks, with each network rendered in a 3D glass brain (semi-transparent) surface model. Note that despite the visualisation, regions belonging to the different RSNs do not overlap, for example, the FPN contains the rostral and caudal middle frontal gyri, whereas the DMN contains the superior and inferior frontal gyri, which are difficult to differentiate in rendered models.

pars opercularis. There were no regions where oxytocin decreased local efficiency.

Details of significant nodal results are presented in Table 2, Fig. 2 and Fig S3.

Subnetworks. The NBS analyses did not identify any subnetworks where there were significant treatment effects on connectivity after correcting for multiple testing, irrespective of the primary threshold used.

Overlap with RSNs. The pathways for which we identified significant nodal modulatory effects of oxytocin overlapped primarily with regions belonging to the ventral attention (Dice coefficient = 0.48) and somatomotor (Dice coefficient = 0.31) networks (Fig. 3).

Interaction effects (group x treatment)
Global metrics. There were no significant interaction effects on mean functional connectivity (t(43) = −0.25, p = 0.80) nor global efficiency (t(43) = −0.85, p = 0.40).

Betweenness-centrality. Significant interaction effects were observed in a number of brain regions. In CHR-P individuals, compared to placebo, oxytocin increased the betweenness-centrality of the left thalamus, right pallidum and right precentral gyrus, whereas in controls, the betweenness-centrality in these regions was decreased after oxytocin. Conversely, in the left nucleus accumbens, left precuneus and left superior frontal gyrus, compared to placebo, oxytocin decreased betweenness-centrality in CHR-P individuals whereas it increased betweenness-centrality in controls.

Nodal degree. Two regions showed significant interaction effects. In CHR-P individuals, relative to placebo, oxytocin decreased node degree of the left precuneus cortex and left superior frontal gyrus, while node degree of these regions increased in controls after oxytocin vs placebo.

Local efficiency. Significant interaction effects were observed for four nodes. In CHR-P individuals, compared to placebo, oxytocin increased the local efficiency of the bilateral entorhinal cortex and right temporal pole. In each of these, oxytocin decreased the local efficiency in controls. The opposite pattern was observed in the left pericalcarine cortex, with oxytocin (vs placebo) decreasing the local efficiency in CHR-P individuals but increasing it in controls.

Details of significant nodal results are presented in Table 2, Fig. 2 and Fig S4.

Subnetworks. The NBS analyses did not identify any subnetworks where there were significant interaction effects on connectivity after correcting for multiple testing, irrespective of the primary threshold used.

Overlap with RSNs. The pathways for which we identified significant nodal interaction effects overlapped primarily with regions belonging to the default-mode network (Dice coefficient = 0.35; Fig. 3).

Further supplemental analyses
Supplemental analyses of global and nodal metrics using partial correlation matrices are appended in the Supplementary Material.

DISCUSSION
Using a data-driven approach, we investigated differences in the topology of the functional connectome—at multiple levels of its hierarchical organisation—in people at CHR-P and examined whether intranasal oxytocin might attenuate some of these differences. We first demonstrated that (a) CHR-P individuals exhibit predominantly greater local graph metrics compared to healthy controls in regions most localised to the frontoparietal network, while normative global network efficiency appears to be preserved, and (b) that oxytocin mainly produced increases in local graph metrics, predominantly in the ventral attention network. The major—and novel—finding of the current study was that many effects of oxytocin on network topology differ across CHR-P and healthy individuals, with significant interaction effects observed in numerous brain regions strongly implicated in psychosis onset, which localised primarily to the default mode network. Collectively, these findings provide new insights on alterations in functional network organisation associated with psychosis risk. Furthermore, they provide the first in vivo evidence that oxytocin modulates network topology in regions implicated in the pathophysiology of psychosis in a clinical status (CHR-P vs healthy control) specific manner, which strengthens the rationale for future studies investigating the therapeutic role of oxytocin in this clinical population.

Differences in network topology related to CHR-P status
Our first finding was that most differences in local network topology related to CHR-P status (i.e. group effects) reflected greater nodal centrality in patients compared to controls. These effects mapped primarily to the frontoparietal resting state network, a major cognitive control system shown to be impaired in patients across the psychosis continuum [65, 66] and transdiagnostic pathological conditions [67, 68]. Notably, we found greater local efficiency and nodal degree in CHR-P individuals across numerous frontal regions, indexing greater integration and importance of these nodes in the network, respectively [27]. Despite the relatively few studies to have examined graph metrics in CHR-P cohorts to date, our results are supported by previous findings of increased topological centrality [5] and/or altered modular assignment [4, 6] of these regions in CHR-P and established psychosis [32] samples.

Importantly, our group effects emerged against a backdrop of no significant differences in raw connectivity strength, suggesting that these nodal differences may instead be signatures of a reorganisation of the brain's functional network architecture [4, 26]. Whether these changes arise through proximal frontal dysfunction, or reflect compensatory changes in response to dysfunctional network dynamics occurring elsewhere [26], is unclear. Conceptually, however, such reorganisations of network architecture are thought to lead to inefficient information flow, aberrant input integration and manifestation of the psychotic and cognitive symptoms [1, 26, 29] characteristic of the CHR-P state, the latter of which may be particularly relevant given that half of our group differences were localised to the frontal cortex. Conversely, the lack of significant differences we observed in global efficiency suggests that *global* capacity for information transfer may be preserved in our CHR-P sample, although we note that such a lack of significant differences could also occur due to data insensitivity. Nevertheless, our findings here are consistent with some [5] (but not all [6]) previous literature, including a large multi-cohort study using age-matched controls across the psychosis spectrum [34]. Together, these findings lend support to the idea that the connectomic dysfunction preceding psychosis onset may be more subtle and characterised by changes in local functional network architecture [34]. However, future studies with the optimum design to test for group differences are now needed to replicate these results, given the difference in study procedures in the present analysis.

Effects of oxytocin on network topology
We next showed that across all measures of local network topology, oxytocin predominantly increased graph metrics

compared to placebo. Of particular interest was the finding that oxytocin increased betweenness-centrality in the brainstem. High betweenness-centrality reflects nodes that participate in a large number of shortest paths in the network, thereby acting as 'bridging nodes' that mediate information flow and network integration [27]. Our findings accord with those in a previous overlapping study in healthy controls, where oxytocin increased the nodal degree—an index of the importance of a node, equal to its number of edges—also in the brainstem [45]. The brainstem is considered a key autonomic hub in models of dopamino-oxytocinergic-mediated social and emotional cognition [69], is a purported substrate for salience detection [70] (through connections with the ventral tegmental area [VTA] and mesolimbic dopamine pathway [71]) and is one potential mediator of the tuning effects of oxytocin on these processes [70]. Consistent with this, we found that oxytocin-induced changes in graph metrics mapped primarily onto the ventral attention network [64], an aggregate of the salience network and the site of the strongest effects of oxytocin on timeseries connectivity in a previous report [41]. Considering that our results were derived after collapsing across healthy controls and CHR-P individuals, effects of oxytocin within the ventral attention network, brainstem and other regions found here could be said to reflect common effects that operate irrespective of clinical status.

Group x treatment interaction effects

Our major—and to our knowledge, novel—finding was the presence of widespread interaction effects across all local graph metrics and across a multitude of brain regions, suggesting that oxytocin modulates network properties in a clinical status-specific manner. This is consistent with the differential effects of oxytocin on timeseries correlational connectivity reported in a variety of clinical populations vs healthy controls, including patients with social anxiety [42], post-traumatic stress disorder [43] and autism [44]. Here we demonstrate, for the first time, that this is also the case in terms of effects on functional brain network topology in people at CHR-P.

Strikingly, oxytocin was found to have divergent effects on local topology in core regions implicated in the pathophysiology of psychosis, including betweenness-centrality of the thalamus and striatum (pallidum, nucleus accumbens [NAcc]), and local efficiency of the entorhinal cortex. In all of these regions except the NAcc, graph metrics were relatively lower in CHR-P individuals under placebo and were increased by oxytocin, with the reverse relationship seen in controls. The thalamus, hippocampus and striatum (including pallidum and NAcc) represent key components of the most influential circuit models of psychosis, which propose that hippocampal hyperactivation drives downstream striatal hyperdopaminergia via increased excitation of the NAcc, increased inhibition of ventral pallidum and thus reduced inhibition of midbrain/VTA dopamine neurons projecting to the NAcc and associative striatum [15–17]. Given the well-established dysfunction within these regions in psychosis, one possibility is that oxytocin's effects differ as a function of baseline network (dis)organisation. Nonpsychotic first-degree relatives have abnormal anatomic centrality in many of the regions reported here, including the pallidum, thalamus and hippocampus [72]. Although we did not find significant effects in the hippocampus directly, the entorhinal cortex is part of the hippocampal formation and acts as a multilevel buffer, bi-directionally gating information flow between neocortex and hippocampus [73]. Reduced nodal clustering has been observed in the hippocampus, thalamus and amygdala in CHR-P transitions vs non-transitions and controls [6], and adolescent-onset schizophrenia patients show decreased nodal efficiency and strength within highly integrative network hubs, most consistently in the hippocampal formation [2]. Transition to psychosis is also associated with reduced thalamic efficiency [6] and thalamocortical dysconnectivity more broadly [20]. If, as this evidence suggests, network topology is altered in CHR-P individuals, it is conceivable that the net effects of exogenously administered oxytocin on network organisation may well differ, even if its cognitive-behavioural effects are still geared towards optimised tuning of social salience/attentional orientation [74]. Such interaction effects would echo those seen among the wider connectivity literature [75, 76] where the greatest magnitude of the connectomic, cognitive and/or behavioural effects of oxytocin are often reported in those subjects with the greatest divergence (compared to controls) at baseline/under placebo [42, 76]. Future studies could explore whether this is also the case in CHR-P and examine whether the effects of oxytocin on neurochemical metabolites [38] are related to its network-level effects, similar to what has been reported (using task-based fMRI) in autism [77], which would provide insight into underlying mechanisms.

Albeit in the context of interactions, in contrast to the other subcortical interaction effects we found relatively *greater* centrality of the NAcc in the CHR-P group under placebo, a region previously identified as a locus of CHR-associated structural rich-club dysfunction [78]. The NAcc is also the terminus for dopamine neurons projecting from the midbrain/VTA [79] in the above-mentioned psychosis-linked circuit. Although speculative, our finding that in CHR-P patients, oxytocin decreased the centrality of the NAcc but increased centrality of the pallidum (which provides inhibition of the VTA) may suggest that oxytocin affects network properties—in mesolimbic dopamine pathway regions—in a psychosis risk-selective manner, and in a direction that ameliorates baseline dysfunction. Indeed, engagement of dopaminergic circuits seems to be a key locus for some of the effects of oxytocin [80] (for a review see [81]) and a wealth of evidence demonstrates interplay of the dopamine and oxytocin systems [82–85]. Overall, psychosis risk-related differences in network topology, dopamine function, the oxytocin system [47], as well as alterations in the set-points of other circuits are not mutually exclusive and may each contribute to the differential net effects of oxytocin on graph properties observed here.

Limitations

A number of limitations warrant consideration. First, data from CHR-P and healthy control groups were from different studies that had slightly different experimental designs, with the controls participating in a triple-dummy study (using multiple administration methods on all occasions) and CHR-P subjects participating in a simple oxytocin vs placebo nasal spray challenge. While the two studies were conceived together specifically to ensure that their data could be combined for the present analyses, it is possible that residual effects from differing designs (for example, from the numerous placebo conditions in the control group, and differential expectation effects in the patients vs controls) could underlie some of the group differences we observed. Our group effects should therefore be interpreted with caution until they can be replicated by future studies optimally designed to test this hypothesis. Second, we did not pre-register an analysis plan, which has become a principle of open science and reduces researcher degrees of freedom. However, as an exploratory, data-driven study, we did not specify hypotheses beyond the standard contrasts (main effects of group, treatment and interactions) and we used the same graph indices as our previously published healthy control study [45]. Third, a number of the clinical and demographic variables collected in the CHR-P group were not collected in controls. As we did not control for any such potential confounders within the analyses, we cannot rule out an effect on our between-group results. Our sample size was relatively large for pharmaco-MRI study including a CHR-P sample, but a recent paper on the reliability of graph analytic results suggested that sample sizes of more than 80 are needed [86]. However, as well as

collecting multi-echo data we used a rigorous denoising protocol (ME-ICA) with enhanced quality control procedures, a combination that has been shown to perform favourably in terms of signal-to-noise ratio compared to other denoising pipelines [53]. We further sought to maximise reliability of our findings by using weighted graphs and metrics summarised (using AUC) across multiple cost functions.

A further consideration is the impact that different preprocessing/analytical pipelines have on graph theoretical measures and neuroimaging results more broadly [59]. For example, a wide variety of parcellation atlases now exist [87] and there is much ongoing debate [88] around the appropriateness [89] (or lack thereof [90]) of global signal regression—especially when combined with ME-ICA—as well as on the relative advantages of full vs partial correlation measures, particularly for mitigating the effects of head motion [91–93]. However, the decision to use one approach vs another is more likely a question of usefulness for the research question, with the various pipelines providing complementary insights [88]. Going forward, further work is required to establish the impact (and optimal combination) of methodological choices on the robustness, reliability and usefulness of network-based metrics, such as those used in the current study.

A final consideration is that our findings may be specific to the mid-to-high range dose (40IU) of oxytocin, male sex, regime of administration (single) and time post-dosing used in this study. Importantly, since designing our study there has been increased understanding of the inverted-U dose-response pharmacodynamic effects of intranasal oxytocin, and indeed we [94] (and others) have since shown that lower doses may be more efficacious for various outcomes [95–98]. It is therefore possible that our 40IU dose was higher than the optimal dose for connectomic and other neurophysiological effects. However, given that different brain regions—and indeed different neural/biological parameters—are likely to have differing dose-response curves [94–98], which may also differ between specific clinical and healthy populations (e.g. due to regional differences in oxytocin receptor expression [99]), we took a pragmatic approach based on our earlier research in healthy controls [49]. In doing so, the current study provides the first evidence that oxytocin does modulate the functional connectome in CHR-P patients, and provides the rationale for future studies now seeking to unravel whether and how such effects differ (and can be optimised) by dose, timing interval and the clinical population under study.

CONCLUSIONS
Collectively, our findings provide new insights on aberrant functional brain network organisation associated with psychosis risk and demonstrate, for the first time, that oxytocin modulates network topology in brain regions implicated in the pathophysiology of psychosis in a clinical status-specific manner. However, it should be noted that our data were derived from two studies with different designs, and thus these results require replication. Nevertheless, given the current lack of effective treatments for people at CHR-P, a deeper understanding of how functional connectomic alterations contribute to psychosis risk and onset, and the potential ameliorative effects of experimental therapeutics such as oxytocin, remain important avenues for future research.

DATA AVAILABILITY
The datasets generated and analysed during the current study are not publicly available due to reasons of data privacy and regulatory/ethical approvals, but aggregate-level data are available from the corresponding author upon reasonable request and pending local and national data protection and ethics regulations.

REFERENCES
1. Collin G, Keshavan MS. Connectome development and a novel extension to the neurodevelopmental model of schizophrenia. Dialog Clin Neurosci. 2018;20:101–11.
2. Li M, Becker B, Zheng J, Zhang Y, Chen H, Liao W, et al. Dysregulated maturation of the functional connectome in antipsychotic-naïve, first-episode patients with adolescent-onset schizophrenia. Schizophrenia Bull. 2019;45:689–97.
3. Morgan SE, Young J, Patel AX, Whitaker KJ, Scarpazza C, van Amelsvoort T, et al. Functional magnetic resonance imaging connectivity accurately distinguishes cases with psychotic disorders from healthy controls, based on cortical features associated with brain network development. Biol Psychiatry. 2021;6:1125–34.
4. Collin G, Seidman LJ, Keshavan MS, Stone WS, Qi Z, Zhang T, et al. Functional connectome organization predicts conversion to psychosis in clinical high-risk youth from the SHARP program. Mol Psychiatry. 2020;25:2431–40.
5. Lord LD, Allen P, Expert P, Howes O, Broome M, Lambiotte R, et al. Functional brain networks before the onset of psychosis: a prospective fMRI study with graph theoretical analysis. NeuroImage: Clin. 2012;1:91–8.
6. Wang C, Lee J, Ho NF, Lim JKW, Poh JS, Rekhi G, et al. Large-scale network topology reveals heterogeneity in individuals with at risk mental state for psychosis: Findings from the longitudinal youth-at-risk study. Cereb Cortex. 2018;28:4234–43.
7. Fusar-Poli P, Salazar De Pablo G, Correll CU, Meyer-Lindenberg A, Millan MJ, Borgwardt S, et al. Prevention of Psychosis: Advances in Detection, Prognosis, and Intervention. JAMA Psychiatry. 2020;77:755–65.
8. Salazar De Pablo G, Radua J, Pereira J, Bonoldi I, Arienti V, Besana F, et al. Probability of transition to psychosis in individuals at clinical high risk: an updated meta-analysis. JAMA Psychiatry. 2021;78:970–8.
9. Davies C, Cipriani A, Ioannidis JPA, Radua J, Stahl D, Provenzani U, et al. Lack of evidence to favor specific preventive interventions in psychosis: a network meta-analysis. World Psychiatry. 2018;17:196–209.
10. Davies C, Radua J, Cipriani A, Stahl D, Provenzani U, McGuire P, et al. Efficacy and acceptability of interventions for attenuated positive psychotic symptoms in individuals at clinical high risk of psychosis: a network meta-analysis. Front Psychiatry. 2018;9:1–17.
11. Allen P, Luigjes J, Howes OD, Egerton A, Hirao K, Valli I, et al. Transition to psychosis associated with prefrontal and subcortical dysfunction in ultra high-risk individuals. Schizophrenia Bull. 2012;38:1268–76.
12. Jalbrzikowski M, Hayes RA, Wood SJ, Nordholm D, Zhou JH, Fusar-Poli P, et al. Association of structural magnetic resonance imaging measures with psychosis onset in individuals at clinical high risk for developing psychosis: an ENIGMA working group mega-analysis. JAMA Psychiatry. 2021;78:753–66.
13. Lieberman JA, Small SA, Girgis RR. Early detection and preventive intervention in schizophrenia: From fantasy to reality. Am J Psychiatry. 2019;176:794–810.
14. Andreou C, Borgwardt S. Structural and functional imaging markers for susceptibility to psychosis. Mol Psychiatry. 2020;25:2773–85.
15. Lisman JE, Coyle JT, Green RW, Javitt DC, Benes FM, Heckers S, et al. Circuit-based framework for understanding neurotransmitter and risk gene interactions in schizophrenia. Trends Neurosci. 2008;31:234–42.
16. Grace AA, Gomes FV. The circuitry of dopamine system regulation and its disruption in schizophrenia: insights into treatment and prevention. Schizophrenia Bull. 2019;45:148–57.
17. Dandash O, Pantelis C, Fornito A. Dopamine, fronto-striato-thalamic circuits and risk for psychosis. Schizophrenia Res. 2017;180:48–57.
18. Fornito A, Harrison BJ, Goodby E, Dean A, Ooi C, Nathan PJ, et al. Functional dysconnectivity of corticostriatal circuitry as a risk phenotype for psychosis. JAMA Psychiatry. 2013;70:1143–51.
19. Colibazzi T, Yang Z, Horga G, Yan CG, Corcoran CM, Klahr K, et al. Aberrant temporal connectivity in persons at clinical high risk for psychosis. Biol Psychiatry: Cogn Neurosci Neuroimaging. 2017;2:696–705.
20. Anticevic A, Haut K, Murray JD, Repovs G, Yang GJ, Diehl C, et al. Association of thalamic dysconnectivity and conversion to psychosis in youth and young adults at elevated clinical risk. JAMA Psychiatry. 2015;72:882–91.
21. O'Neill A, Mechelli A, Bhattacharyya S. Dysconnectivity of large-scale functional networks in early psychosis: a meta-analysis. Schizophrenia Bull. 2019;45:579–90.
22. Wotruba D, Michels L, Buechler R, Metzler S, Theodoridou a, Gerstenberg M, et al. Aberrant Coupling Within and Across the Default Mode, Task-Positive, and Salience Network in Subjects at Risk for Psychosis. Schizophrenia Bulletin. 2014;40:1095–1104.
23. Del Fabro L, Schmidt A, Fortea L, Delvecchio G, D'Agostino A, Radua J, et al. Functional brain network dysfunctions in subjects at high-risk for psychosis: a meta-analysis of resting-state functional connectivity. Neurosci Biobehav Rev. 2021;128:90–101.
24. Watts DJ, Strogatz SH. Collective dynamics of 'small-world' networks. Nature. 1998;393:440–2.

25. Bullmore ET, Bassett DS. Brain graphs: Graphical models of the human brain connectome. Annu Rev Clin Psychol. 2011;7:113–40.

26. Fornito A, Zalesky A, Pantelis C, Bullmore ET. Schizophrenia, neuroimaging and connectomics. NeuroImage. 2012;62:2296–314.

27. Rubinov M, Sporns O. Complex network measures of brain connectivity: uses and interpretations. NeuroImage. 2010;52:1059–69.

28. Collin G, Scholtens LH, Kahn RS, Hillegers MHJ, van den Heuvel MP. Affected anatomical rich club and structural–functional coupling in young offspring of schizophrenia and bipolar disorder patients. Biol Psychiatry. 2017;82:746–55.

29. Friston K, Brown HR, Siemerkus J, Stephan KE. The dysconnection hypothesis (2016). Schizophrenia Res. 2016;176:83–94.

30. Kambeitz J, Kambeitz-Ilankovic L, Cabral C, Dwyer DB, Calhoun VD, Van Den Heuvel MP, et al. Aberrant functional whole-brain network architecture in patients with schizophrenia: a meta-analysis. Schizophrenia Bull. 2016;42:S13–21.

31. Liu Y, Liang M, Zhou Y, He Y, Hao Y, Song M, et al. Disrupted small-world networks in schizophrenia. Brain. 2008;131:945–61.

32. Lynall ME, Bassett DS, Kerwin R, McKenna PJ, Kitzbichler M, Muller U, et al. Functional connectivity and brain networks in schizophrenia. J Neurosci. 2010;30:9477–87.

33. Alexander-Bloch AF, Gogtay N, Meunier D, Birn R, Clasen L, Lalonde F, et al. Disrupted modularity and local connectivity of brain functional networks in childhood-onset schizophrenia. Front Syst Neurosci. 2010;4:1–16.

34. Jalbrzikowski M, Liu F, Foran W, Roeder K, Devlin B, Luna B. Resting-state functional network organization is stable across adolescent development for typical and psychosis spectrum youth. Schizophrenia Bull. 2020;46:395–407.

35. Smith AS, Tabbaa M, Lei K, Eastham P, Butler MJ, Linton L, et al. Local oxytocin tempers anxiety by activating GABAA receptors in the hypothalamic paraventricular nucleus. Psychoneuroendocrinology. 2016;63:50–8.

36. Meyer-Lindenberg A, Domes G, Kirsch P, Heinrichs M. Oxytocin and vasopressin in the human brain: social neuropeptides for translational medicine. Nat Rev Neurosci. 2011;12:524–38.

37. Schmidt A, Davies C, Paloyelis Y, Meyer N, De Micheli A, Ramella-Cravaro V, et al. Acute oxytocin effects in inferring others' beliefs and social emotions in people at clinical high risk for psychosis. Transl Psychiatry. 2020;10:203.

38. Davies C, Rutigliano G, De Micheli A, Stone JM, Ramella-Cravaro V, Provenzani U, et al. Neurochemical effects of oxytocin in people at clinical high risk for psychosis. Eur Neuropsychopharmacol. 2019;29:601–15.

39. Davies C, Paloyelis Y, Rutigliano G, Cappucciati M, De Micheli A, Ramella-Cravaro V, et al. Oxytocin modulates hippocampal perfusion in people at clinical high risk for psychosis. Neuropsychopharmacology. 2019;44:1300–9.

40. Xin F, Zhou F, Zhou X, Ma X, Geng Y, Zhao W, et al. Oxytocin modulates the intrinsic dynamics between attention-related large-scale networks. Cerebral Cortex. 2021;31:1848–60.

41. Brodmann K, Gruber O, Goya-Maldonado R. Intranasal oxytocin selectively modulates large-scale brain networks in humans. Brain Connectivity. 2017;7:brain.2017.0528.

42. Dodhia S, Hosanagar A, Fitzgerald DA, Labuschagne I, Wood AG, Nathan PJ, et al. Modulation of resting-state amygdala-frontal functional connectivity by oxytocin in generalized social anxiety disorder. Neuropsychopharmacology. 2014;39:2061–9.

43. Koch SB, van Zuiden M, Nawijn L, Frijling JL, Veltman DJ, Olff M. Intranasal oxytocin normalizes amygdala functional connectivity in post-traumatic stress disorder. Neuropsychopharmacology. 2016;41:1–34.

44. Procyshyn TL, Lombardo MV, Lai MC, Jassim N, Auyeung B, Crockford SK, et al. Oxytocin enhances basolateral amygdala activation and functional connectivity while processing emotional faces: preliminary findings in autistic versus non-autistic women. Soc Cognit Affect Neurosci. 2022;17:929–38.

45. Martins D, Dipasquale O, Paloyelis Y. Oxytocin modulates local topography of human functional connectome in healthy men at rest. Commun Biol. 2021;4:68.

46. Owen SF, Tuncdemir SN, Bader PL, Tirko NN, Fishell G, Tsien RW. Oxytocin enhances hippocampal spike transmission by modulating fast-spiking interneurons. Nature. 2013;500:458–62.

47. Shilling PD, Feifel D. Potential of oxytocin in the treatment of schizophrenia. CNS Drugs. 2016;30:193–208.

48. Martins D, Davies C, Micheli A, De, Oliver D, Fusar-poli P, et al. Intranasal oxytocin increases heart-rate variability in men at clinical high risk for psychosis: a proof-of-concept study. Transl Psychiatry. 2020;10:227.

49. Paloyelis Y, Doyle OM, Zelaya FO, Maltezos S, Williams SC, Fotopoulou A, et al. A spatiotemporal profile of in vivo cerebral blood flow changes following intranasal oxytocin in humans. Biol Psychiatry. 2016;79:693–705.

50. Guastella AJ, Hickie IB, McGuinness MM, Otis M, Woods EA, Disinger HM, et al. Recommendations for the standardisation of oxytocin nasal administration and guidelines for its reporting in human research. Psychoneuroendocrinology. 2013;38:612–25.

51. Kagerbauer SM, Debus JM, Martin J, Gempt J, Jungwirth B, Hapfelmeier A, et al. Absence of a diurnal rhythm of oxytocin and arginine-vasopressin in human cerebrospinal fluid, blood and saliva. Neuropeptides. 2019;78:101977.

52. Kundu P, Brenowitz ND, Voon V, Worbe Y, Vértes PE, Inati SJ, et al. Integrated strategy for improving functional connectivity mapping using multiecho fMRI. Proc Natl Acad Sci USA. 2013;110:16187–92.

53. Dipasquale O, Sethi A, Lagan MM, Baglio F, Baselli G, Kundu P, et al. Comparing resting state fMRI de-noising approaches using multi-and single-echo acquisitions. PLoS ONE. 2017;12:1–25.

54. Desikan RS, Ségonne F, Fischl B, Quinn BT, Dickerson BC, Blacker D, et al. An automated labeling system for subdividing the human cerebral cortex on MRI scans into gyral based regions of interest. NeuroImage. 2006;31:968–80.

55. Martins D, Dipasquale O, Davies K, Cooper E, Tibble J, Veronese M, et al. Transcriptomic and cellular decoding of functional brain connectivity changes reveal regional brain vulnerability to pro- and anti-inflammatory therapies. Brain Behav Immun. 2022;102:312–23.

56. Dipasquale O, Cohen A, Martins D, Zelaya F, Turkheimer F, Veronese M, et al. Molecular-enriched functional connectivity in the human brain using multiband multi-echo simultaneous ASL/BOLD fMRI. Sci Rep. 2023;13:11751.

57. Jacob Y, Morris LS, Huang KH, Schneider M, Rutter S, Verma G, et al. Neural correlates of rumination in major depressive disorder: A brain network analysis. NeuroImage: Clin. 2020;25:102142.

58. Martins D, Giacomel A, Williams SCR, Turkheimer F, Dipasquale O, Veronese M. Imaging transcriptomics: convergent cellular, transcriptomic, and molecular neuroimaging signatures in the healthy adult human brain. Cell Rep. 2021;37:110173.

59. Pervaiz U, Vidaurre D, Woolrich MW, Smith SM. Optimising network modelling methods for fMRI. NeuroImage. 2020;211:116604.

60. van den Heuvel MP, de Lange SC, Zalesky A, Seguin C, Yeo BTT, Schmidt R. Proportional thresholding in resting-state fMRI functional connectivity networks and consequences for patient-control connectome studies: Issues and recommendations. NeuroImage. 2017;152:437–49.

61. Achard S, Bullmore E. Efficiency and cost of economical brain functional networks. PLoS Comput Biol. 2007;3:0174–83.

62. Zhang J, Wang J, Wu Q, Kuang W, Huang X, He Y, et al. Disrupted brain connectivity networks in drug-naive, first-episode major depressive disorder. Biol Psychiatry. 2011;70:334–42.

63. Zalesky A, Fornito A, Bullmore ET. Network-based statistic: Identifying differences in brain networks. NeuroImage. 2010;53:1197–207.

64. Yeo BTT, Krienen FM, Sepulcre J, Sabuncu MR, Lashkari D, Hollinshead M, et al. The organization of the human cerebral cortex estimated by intrinsic functional connectivity. J Neurophysiol. 2011;106:1125–65.

65. Satterthwaite TD, Baker JT. How can studies of resting-state functional connectivity help us understand psychosis as a disorder of brain development? Curr Opin Neurobiol. 2015;30:85–91.

66. Schmidt A, Diwadkar VA, Smieskova R, Harrisberger F, Lang UE, McGuire P, et al. Approaching a network connectivity-driven classification of the psychosis continuum: A selective review and suggestions for future research. Front Hum Neurosci. 2015;8:1–16.

67. Baker JT, Dillon DG, Patrick LM, Roffman JL, Brady RO, Pizzagalli DA, et al. Functional connectomics of affective and psychotic pathology. Proc Natl Acad Sci USA. 2019;116:9050–9.

68. Sha Z, Wager TD, Mechelli A, He Y. Common dysfunction of large-scale neurocognitive networks across psychiatric disorders. Biol Psychiatry. 2019;85:379–88.

69. Rosenfeld AJ, Lieberman JA, Jarskog LF. Oxytocin, dopamine, and the amygdala: A neurofunctional model of social cognitive deficits in schizophrenia. Schizophrenia Bull. 2011;37:1077–87.

70. Shamay-Tsoory SG, Abu-Akel A. The social salience hypothesis of oxytocin. Biol Psychiatry. 2015;79:1–9.

71. Redgrave P, Gurney K. The short-latency dopamine signal: A role in discovering novel actions? Nat Rev Neurosci. 2006;7:967–75.

72. Zhang W, Lei D, Keedy SK, Ivleva EI, Eum S, Yao L, et al. Brain gray matter network organization in psychotic disorders. Neuropsychopharmacology. 2020;45:666–74.

73. Small SA, Schobel SA, Buxton RB, Witter MP, Barnes CA. A pathophysiological framework of hippocampal dysfunction in ageing and disease. Nat Rev Neurosci. 2011;12:585–601.

74. Ma Y, Shamay-Tsoory S, Han S, Zink CF. Oxytocin and social adaptation: insights from neuroimaging studies of healthy and clinical populations. Trends Cogn Sci. 2016;20:133–45.

75. Choe KY, Bethlehem RAI, Safrin M, Dong H, Salman E, Li Y, et al. Oxytocin normalizes altered circuit connectivity for social rescue of the Cntnap2 knockout mouse. Neuron. 2022;110:795–808.

76. Abram SV, De Coster L, Roach BJ, Mueller BA, van Erp TGM, Calhoun VD, et al. Oxytocin enhances an amygdala circuit associated with negative symptoms in

schizophrenia: a single-dose, placebo-controlled, crossover, randomized control trial. Schizophrenia Bull. 2020;46:661–69.

77. Aoki Y, Watanabe T, Abe O, Kuwabara H, Yahata N, Takano Y, et al. Oxytocin's neurochemical effects in the medial prefrontal cortex underlie recovery of task-specific brain activity in autism: a randomized controlled trial. Mol Psychiatry. 2015;20:447–53.

78. Schmidt A, Crossley NA, Harrisberger F, Smieskova R, Lenz C, Riecher-Rössler A, et al. Structural network disorganization in subjects at clinical high risk for psychosis. Schizophrenia Bull. 2017;43:583–91.

79. McCutcheon RA, Abi-dargham A, Howes OD. Schizophrenia, dopamine and the striatum: from biology to symptoms. Trends Neurosci. 2019;42:205–20.

80. Hung LW, Neuner S, Polepalli JS, Beier KT, Wright M, Walsh JJ, et al. Gating of social reward by oxytocin in the ventral tegmental area. Science. 2017;357:1406–11.

81. Love TM. Oxytocin, motivation and the role of dopamine. Pharmacol Biochem Behav. 2014;119:49–60.

82. Rokicki J, Kaufmann T, de Lange AMG, van der Meer D, Bahrami S, Sartorius AM, et al. Oxytocin receptor expression patterns in the human brain across development. Neuropsychopharmacology. 2022;47:1550–60.

83. Quintana DS, Rokicki J, van der Meer D, Alnæs D, Kaufmann T, Córdova-Palomera A, et al. Oxytocin pathway gene networks in the human brain. Nat Commun. 2019;10:668.

84. Romero-Fernandez W, Borroto-Escuela DO, Agnati LF, Fuxe K. Evidence for the existence of dopamine d2-oxytocin receptor heteromers in the ventral and dorsal striatum with facilitatory receptor–receptor interactions. Mol Psychiatry. 2012;18:849–50.

85. Love TM, Enoch MA, Hodgkinson CA, Peciña M, Mickey B, Koeppe RA, et al. Oxytocin gene polymorphisms influence human dopaminergic function in a sex-dependent manner. Biol Psychiatry. 2012;72:198–206.

86. Termenon M, Jaillard A, Delon-Martin C, Achard S. Reliability of graph analysis of resting state fMRI using test-retest dataset from the Human Connectome Project. NeuroImage. 2016;142:172–87.

87. Revell AY, Silva AB, Arnold TC, Stein JM, Das SR, Shinohara RT, et al. A framework For brain atlases: lessons from seizure dynamics. NeuroImage. 2022;254:118986.

88. Murphy K, Fox MD. Towards a consensus regarding global signal regression for resting state functional connectivity MRI. NeuroImage. 2017;154:169–73.

89. Power JD, Plitt M, Gotts SJ, Kundu P, Voon V, Bandettini PA, et al. Ridding fMRI data of motion-related influences: Removal of signals with distinct spatial and physical bases in multiecho data. Proc Natl Acad Sci. 2018;115:E2105–14.

90. Spreng RN, Fernández-Cabello S, Turner GR, Stevens WD. Take a deep breath: Multiecho fMRI denoising effectively removes head motion artifacts, obviating the need for global signal regression. Proc Natl Acad Sci. 2019;116:19241–2.

91. Liang X, Wang J, Yan C, Shu N, Xu K, Gong G, et al. Effects of different correlation metrics and preprocessing factors on small-world brain functional networks: a resting-state functional MRI study. PLOS ONE. 2012;7:e32766.

92. Power JD, Schlaggar BL, Petersen SE. Recent progress and outstanding issues in motion correction in resting state fMRI. NeuroImage. 2015;105:536–51.

93. Mahadevan AS, Tooley UA, Bertolero MA, Mackey AP, Bassett DS. Evaluating the sensitivity of functional connectivity measures to motion artifact in resting-state fMRI data. NeuroImage. 2021;241:118408.

94. Martins D, Brodmann K, Veronese M, Dipasquale O, Mazibuko N, Schuschnig U, et al. Less is more": A dose-response account of intranasal oxytocin pharmacodynamics in the human brain. Prog Neurobiol. 2022;211:102239.

95. Spengler FB, Schultz J, Scheele D, Essel M, Maier W, Heinrichs M, et al. Kinetics and dose dependency of intranasal oxytocin effects on amygdala reactivity. Biol Psychiatry. 2017;82:885–94.

96. Lieberz J, Scheele D, Spengler FB, Matheisen T, Schneider L, Stoffel-Wagner B, et al. Kinetics of oxytocin effects on amygdala and striatal reactivity vary between women and men. Neuropsychopharmacol. 2020;45:1134–40.

97. Yamasue H, Kojima M, Kuwabara H, Kuroda M, Matsumoto K, Kanai C, et al. Effect of a novel nasal oxytocin spray with enhanced bioavailability on autism: a randomized trial. Brain. 2022;145:490–9.

98. Quintana DS, Westlye LT, Alnæs D, Rustan ØG, Kaufmann T, Smerud KT, et al. Low dose intranasal oxytocin delivered with Breath Powered device dampens amygdala response to emotional stimuli: a peripheral effect-controlled within-subjects randomized dose-response fMRI trial. Psychoneuroendocrinology. 2016;69:180–8.

99. Uhrig S, Hirth N, Broccoli L, von Wilmsdorff M, Bauer M, Sommer C, et al. Reduced oxytocin receptor gene expression and binding sites in different brain regions in schizophrenia: a post-mortem study. Schizophrenia Res. 2016;177:59–66.

100. Alexander-Bloch AF, Shou H, Liu S, Satterthwaite TD, Glahn DC, Shinohara RT, et al. On testing for spatial correspondence between maps of human brain structure and function. NeuroImage. 2018;178:540–51.

COMPETING INTERESTS
PFP has received research funds or personal fees from Lundbeck, Angelini, Menarini, Sunovion, Boehringer Ingelheim and Proxymm Science outside of the current study. RAM has received honoraria for educational talks sponsored by Otsuka and Janssen. The authors have declared that there are no conflicts of interest in relation to the subject of this study.

ADDITIONAL INFORMATION
Supplementary information The online version contains supplementary material available at https://doi.org/10.1038/s41380-024-02406-x.

Correspondence and requests for materials should be addressed to Cathy Davies.

Reprints and permission information is available at http://www.nature.com/reprints

Publisher's note Springer Nature remains neutral with regard to jurisdictional claims in published maps and institutional affiliations.